Electronic supplementary information

Quasi-Cu-MOF: Highly improved water stability and electrocatalytic activity toward H_2O_2 reduction in pristine 3D MOFs

Duanping Sun [a,b,*], Linxi Chen [a], Lizhu Zeng [c], Xianhua Shi [a], Jing Lu [a,c,*]

[a] Key Laboratory of New Drug Discovery and Evaluation, Guangdong Provincial Key Laboratory of Pharmaceutical Bioactive Substances, Center for Drug Research and Development, Guangdong Pharmaceutical University, Guangzhou 510006, Guangdong, China

[b] Key Specialty of Clinical Pharmacy, The First Affiliated Hospital of Guangdong Pharmaceutical University, Guangzhou 510699, Guangdong, China

[c] National and Local United Engineering Lab of Druggability and New Drugs Evaluation, School of Pharmaceutical Sciences, Sun Yat-Sen University, Guangzhou 510006, Guangdong, China

* Corresponding authors.

E-mail addresses: sundp@gdpu.edu.cn (D. Sun), lujing28@mail.sysu.edu.cn (J. Lu)

Table of Contents

3. Supplementary References

1. Experimental section

1.1. Reagents and materials

Copper nitrate trihydrate ($Cu(NO_3)_2 \cdot 3H_2O$), trimesic acid ($C_9H_6O_6$, benzene-1,3,5-tricarboxylic acid), zinc nitrate hexahydrate ($Zn(NO_3)_2 \cdot 6H_2O$), 2-methylimidazole, cobalt nitrate hexahydrate ($Co(NO_3)_2 \cdot 6H_2O$), iron chloride hexahydrate ($FeCl_3 \cdot 6H_2O$), benzene-1,4-dicarboxylic acid (H_2BDC), N,N-dimethylformamide (DMF), zirconium chloride ($ZrCl_4$), acetic acid, o-phenylenediamine (OPD), hydrogen peroxide solution (H_2O_2, 30%, w/w), glucose (GLU), ascorbic acid (AA), citric acid (CA), and uric acid (UA) were all purchased from Aladin Chemistry Co., Ltd. (Shanghai, China). Nafion (5%) was bought from Alfa Aesar (United States).

Cell counting kit-8 (CCK-8), calcein-AM/propidium iodide (PI) double staining kit, and dehydrogenate (DHE) solution were purchased from Beyotime Biotechnology (Nanjing, China). Phosphate buffered saline (PBS, 10 mM, pH 7.4) contained 136.7 mM NaCl, 2.7 mM KCl, 8.2 mM Na_2HPO4, and 1.8 mM KH_2PO4. All chemicals were of analytical grade and used without further purification.

1.2. Synthesis of five types of typical MOFs

HKUST-1(Cu) was prepared by reacting copper nitrate and trimesic acid. First, 1.82 g $Cu(NO_3)_2 \cdot 3H_2O$ and 0.875 g benzene-1,3,5-tricarboxylic acid were dissolved in 50 mL absolute methanol under ultrasonication. After that, the copper nitrate solution was transferred into the tricarboxylic acid solution, and the mixed solution was sonicated in an ultrasonic cleaner for 1 min. The mixture solution was kept at room temperature for 24 h until MOF precipitation finished. The precipitate was retrieved by centrifugation and washed with methanol 2-3 times. Finally, the blue powder of HKUST-1(Cu) was dried in a vacuum at 60 °C for 12 h.

ZIF-8(Zn) was prepared by reacting zinc nitrate and 2-methylimidazole. First, 0.595 g $Zn(NO_3)_2 \cdot 6H_2O$ and 0.6575 g 2-methylimidazole were dissolved in a 50 mL absolute methanol under ultrasonication, respectively. After that, the zinc acetate solution was transferred into the 2-methylimidazole solution and the mixed solution was sonicated in an ultrasonic cleaner for 1 min. The mixture solution was kept at room temperature for 24 h to grow the standard ZIF-8 crystals with typical rhombic dodecahedron morphology. The product was collected by centrifugation and washed with methanol for 2-3 times. At last, the white powder of ZIF-8(Zn) was dried in vacuum at 60 ºC for 12 h.

ZIF-67(Co) was prepared by reacting cobalt nitrate and 2-methylimidazole. First, 0.546 g $Co(NO_3)_2 \cdot 6H_2O$ and 0.616 g 2-methylimidazole were dissolved in a 30 mL absolute methanol under ultrasonication, respectively. After that, the cobalt nitrate hexahydrate solution was transferred into the 2-methylimidazole solution and the mixed solution was sonicated in an ultrasonic cleaner for 1 min. The mixture solution was kept at room temperature for 24 h to grow the standard ZIF-67 crystals. The purple product was collected by centrifugation and washed with methanol for 2-3 times. At last, the powder of ZIF-67(Zn) was dried in vacuum at 60 ºC for 12 h.

MIL-101(Fe) was prepared by reacting iron chloride and H_2BDC with a solvothermal method. In a typical synthesis, 1.352 g $FeCl_3 \cdot 6H_2O$, 0.415 g H_2BDC and 30 mL DMF were well mixed into a 50 mL Teflon-lined stainless steel autoclave and maintained at 120 °C for 24 h. The brown product was collected by centrifugation and washed with DMF, ethanol and ultrapure water for 2-3 times. At last, the powder of MIL-101(Fe) was dried in vacuum at 60 ºC for 12 h.

UiO-66(Zr) was prepared by reacting zirconium chloride and H_2BDC with a solvothermal method. In a typical synthetic process, 0.080 g $ZrCl_4$ and 0.057 g H_2BDC were dissolved in 20 mL DMF by using ultrasound for 10 min. Then 3 mL of acetic acid was added into the solution to tune the morphology of the product. After further 10 min ultrasonic treatment, the obtained homogeneous solution was then transferred into a 40 mL Teflon-lined stainless steel autoclave and maintained at 120 ºC for 24 h. Finally, the products were collected by centrifugation and washed with DMF, ethanol and ultrapure water for 2-3 times. The powder of UiO-66(Zr) was dried in vacuum at 60 ºC for 12 h.

1.3. Synthesis of QHKUST-1

A glass vessel containing the HKUST-1 MOF powder was placed in a tube furnace under ambient air. The calcination experiment was carried out in airflow (50 mL/min) at a heating rate of 10 °C/min using an initial HKUST-1 mass of 50 mg. To investigate the phase after thermal treatment of HKUST-1, the calcination was performed at 200, 250, 300, 350, and 400 °C for 1 h. After confirming the HKUST-1 crystalline phase remained at 250 °C, the isothermal time of calcination was varied to 1, 2, 3, 4, and 5 h to control the distortion of the symmetric Cu dimer in HKUST-1.

1.4. Material characterization

Morphological features of the samples were studied using a field emission scanning electron microscope (SEM, Geminni500, Germany). Transmission electron microscopy (TEM) images were

obtained using a transmission electron microscope (JEM-1400, Japan), which was operated at an accelerating voltage of 200 kV. Fourier transform infra-red (FT-IR) was carried out by using a Fourier transformation infra-red spectrometer (IR, EQUINOX 55, Germany). The crystal phase of the prepared samples was characterized by X-ray diffraction (XRD) with X-ray powder diffractometer (Empyrean, Netherlands). X-ray photoelectron spectroscopy (XPS) for element state investigation was carried out by using a Thermo Scientific source XPS system (ESCALAB 250). Thermal behavior of HKUST-1 according to the temperature was investigated by a thermogravimetry (TG209F1 libra, Germany). Raman analysis was carried out by using a Renishaw microscope (inVia Qontor, England).

1.5. Catalase-like activity of MOFs

First, the catalase-like activity of MOFs was assayed by observing the generation of oxygen (O_2) through the catalytic decomposition of H_2O_2 as the substrate. The solutions in the tubes containing H_2O_2 and different types of MOFs were reacted at 37 °C for 30 min, and the photos were obtained.

Then, the detailed concentrations of H_2O_2 in different reaction conditions were estimated. The calibration curve of absorbance and the concentration of H_2O_2 (1−25 mM) were recorded by monitoring the absorbance at 240 nm with different concentrations of H_2O_2. The H_2O_2 decomposition experiments were studied by adding different types of MOFs (1.0 mg mL^{-1}) into PBS solution containing H_2O_2 (10 mM) at 37 °C. After a period of time, the mixtures were centrifuged, and the ultraviolet–visible (UV-Vis) spectra of the remaining H_2O_2 were recorded on a UV−Vis spectrophotometer (UV-2600, Shimadzu, Japan).

1.6. Peroxidase-like activity of MOFs

The peroxidase-like activity of different types of MOFs was evaluated via the catalytic oxidation of the OPD at the assist of H_2O_2 in 10 mM PBS (pH 7.4). All the catalytic reactions were performed by monitoring the absorbance changes of OPD at 420 nm. In a typical test, chemicals were added into PBS buffer solution (10 mM, pH 7.0) in an order of MOFs, OPD (final concentration 8.0 mM), and H_2O_2 (final concentration 10.0 mM) under 37 °C. The peroxidase-like activities of MOFs were also investigated by varying the concentrations of OPD (1.0, 2.0, 4.0, 6.0, 8.0, and 10.0 mM), and H_2O_2 (1.0, 2.0, 4.0, 6.0, 8.0, and 10.0 mM). The peroxidase-like activities of different types of MOFs were assessed under the same standard conditions.

1.7. Electrochemical characterization of MOFs

All electrochemical measurements were carried out on a CHI 660E electrochemical workstation (Shanghai CHI Instrument Co., China) with a bare or modified glassy carbon electrode (GCE, 3 mm in diameter) as working electrode, a platinum wire as counter electrode, and an Ag/AgCl (with saturated KCl solution) as reference electrode.

First, the bare GCE was polished using 0.05 μm alumina powder, sonicated with ultrapure water and ethanol for 1 min, and dried by nitrogen. The as-prepared MOFs were redispersed in a mixture of solvents containing water and Nafion (5%) (v:v = 1:0.008) to form a 1 mg mL^{-1} solution. Then 10 μL mixture solution of solvents was dropped onto the GCE surface and dried at room temperature, and MOFs modified GCE surface (MOFs/GCE) was obtained. Before experiments, the PBS electrolyte was purged with nitrogen for 15 min to eliminate residential oxygen. Finally, the sensor was tested with optimized condition in 10 mM PBS containing H_2O_2.

Redox characteristics of the electrode interfaces were assessed by cyclic voltammograms (CV) in a 10 mM PBS buffer. The scan rate for the voltammetric measurements was 100 mV s^{-1}. All those CV curves are from the first run of each sample. Amperometric I-t experiment was performed using the modified electrodes with various concentrations of H_2O_2. The potential was kept at −0.55 V and the current versus time was recorded over successive injection of 2 μL aliquots of H_2O_2 in 5 mL 10 mM PBS. The experiment was repeated three times and results are expressed as mean ± standard deviation.

1.8. Dehydrogenate (DHE) fluorescence

Cellular superoxide generation was detected by DHE staining. Reactive oxygen species (ROS) react with DHE to form ethidium, which then binds to nuclear DNA and releases nuclear fluorescence. Briefly, HepG2 cells were incubated with DHE (1:2000) in the dark for 20 min at 37 °C, and then were rinsed in PBS for ROS detection. A fluorescence microscope was used to observe DHE fluorescence.

1.9. Cytotoxicity tests for QHKUST-1-based sensor

To obtain the cytotoxicity of MOFs-based biosensor, HKUST-1 and QHKUST-1 modified electrodes were immersed into cell culture solution after sanitized with alcohol and short UV light exposure. The cells were dyed using Calcein-AM/PI double-stain kit after 24 h sensor immersion. The cytotoxicity was determined by the fluorescent images of the dyed viable and dead cells obtained a fluorescence microscope.

1.10. Real-time monitoring of H2O2 release and drug evaluation

The H9C2 and HeLa cells were grown in 5% CO_2 with the cell culture medium at 37 °C. After growing to 90% confluence, the cells were gently washed with 10 mM PBS for three times. Then, H9C2 and HeLa cells cultured with different concentrations (0.19 and 0.75 μM) of DOX for 24 h were suspended in 10 mM PBS solution, and QHKUST-1/GCE was placed into it for H_2O_2 monitoring. Ascorbic acid (AA) was injected to stimulate cells to produce H_2O_2 and real-time detection of H_2O_2. The amperometric technique was utilized for measuring the current response for H_2O_2 detection by using the modified electrodes.

2. Supplementary Figures and Tables

Table S1 Five types of typical MOFs names and their composition.

Designation	Metal clusters or ions	Organic linkers	Solvent	Conditions	Abbreviation interpretation
HKUST-1	copper nitrate ($Cu(NO_3)_2$)	trimesic acid	methanol	25 °C for 24 h	Hong Kong University of Science and Technology
ZIF-8	zinc nitrate ($Zn(NO_3)_2$)	2-methylimidazole	methanol	25 °C for 24 h	Zeolite Imidazolate Framework
ZIF-67	cobalt nitrate ($Co(NO_3)_2$)	2-methylimidazole	methanol	25 °C for 24 h	Zeolite Imidazolate Framework
MIL-101	iron chloride ($FeCl_3$)	benzene-1,4-dicarboxylic acid (H_2BDC)	DMF	120 °C for 24 h	Materials of Institut Lavoisier
UIO-66	zirconium chloride ($ZrCl_4$)	benzene-1,4-dicarboxylic acid (H_2BDC)	DMF	120 °C for 24 h	Universitetet i Oslo

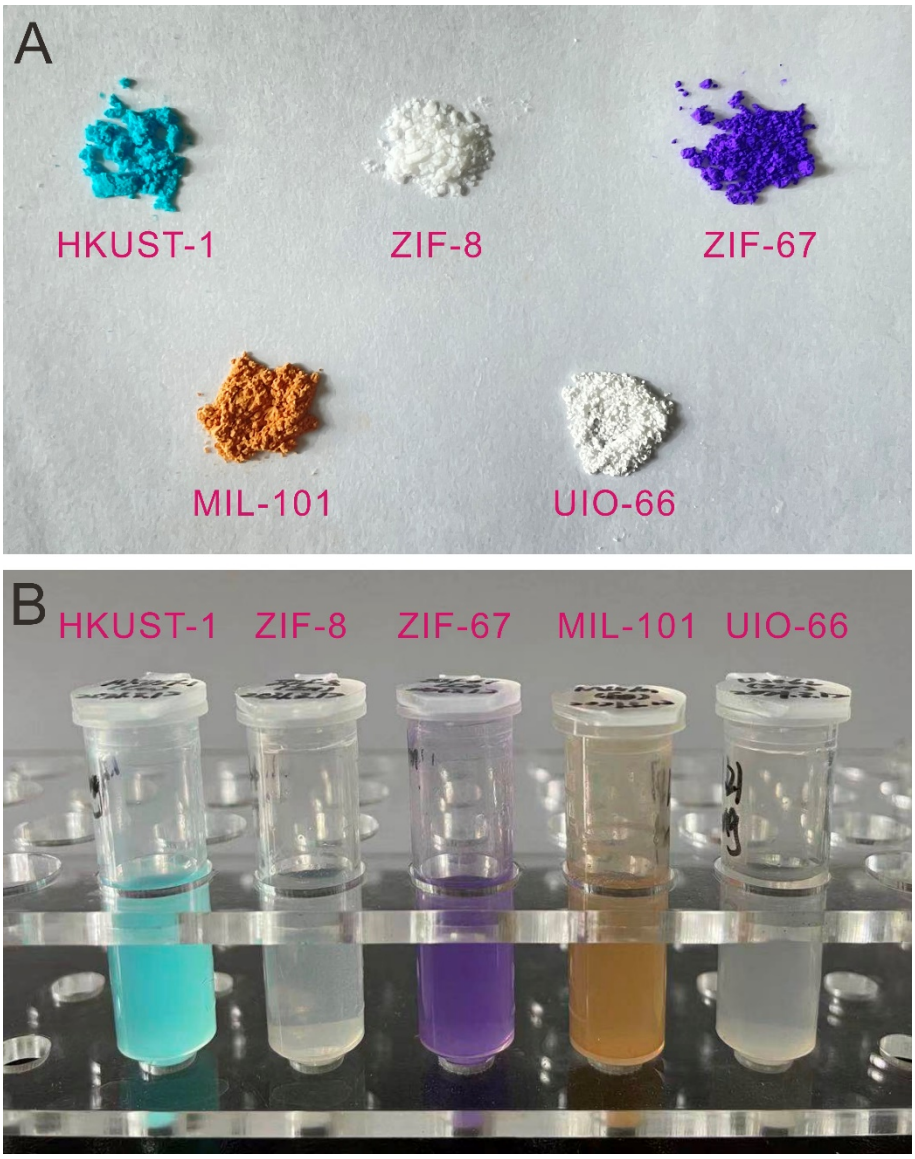

Figure S1. Photographs of five types of MOF powders and MOF water solution in this work.

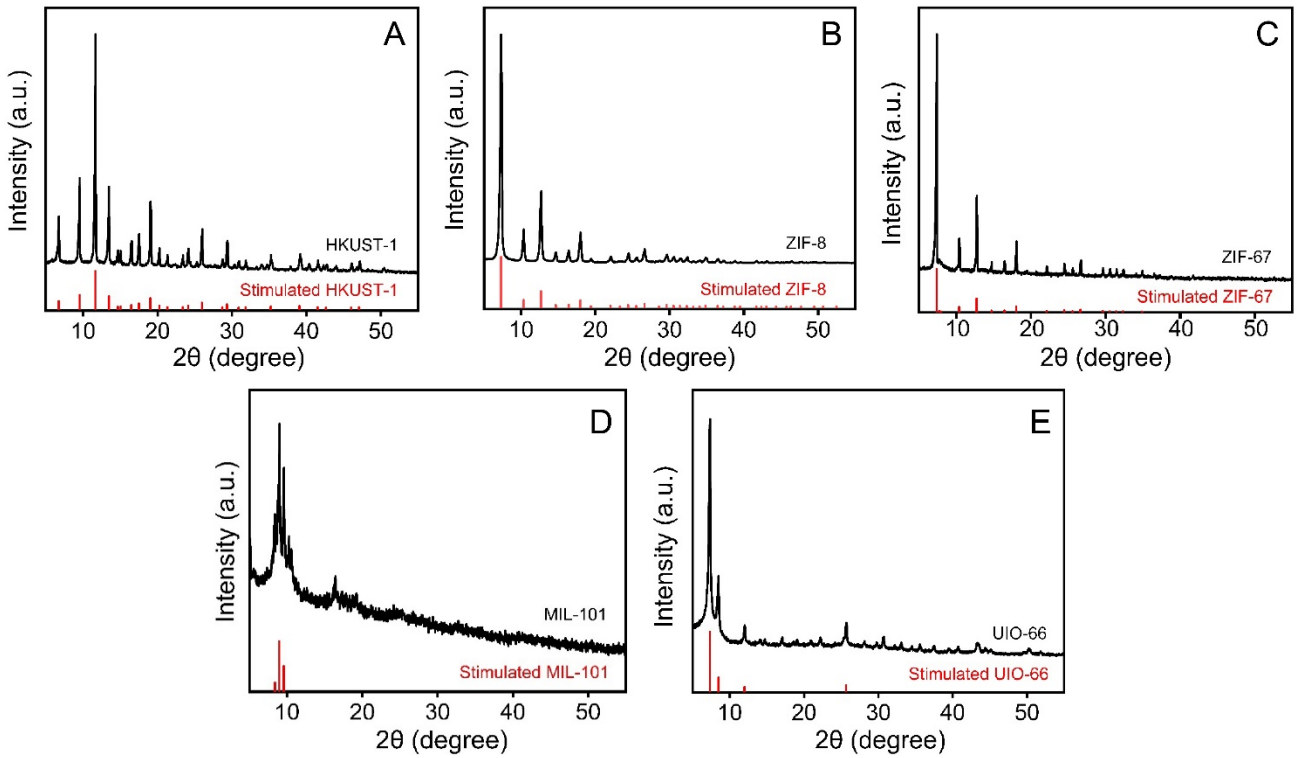

Figure S2. XRD patterns of five types of MOF materials.

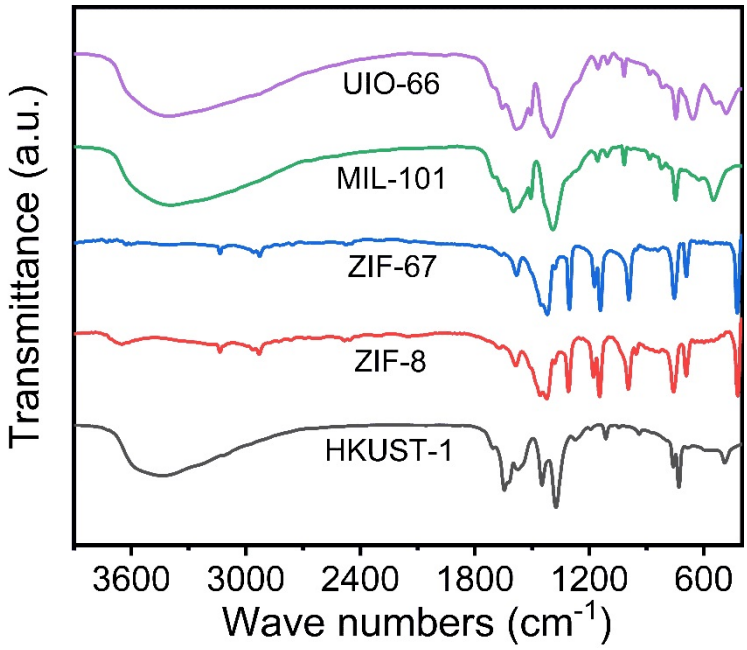

Figure S3. FT-IR spectra of five types of MOF materials.

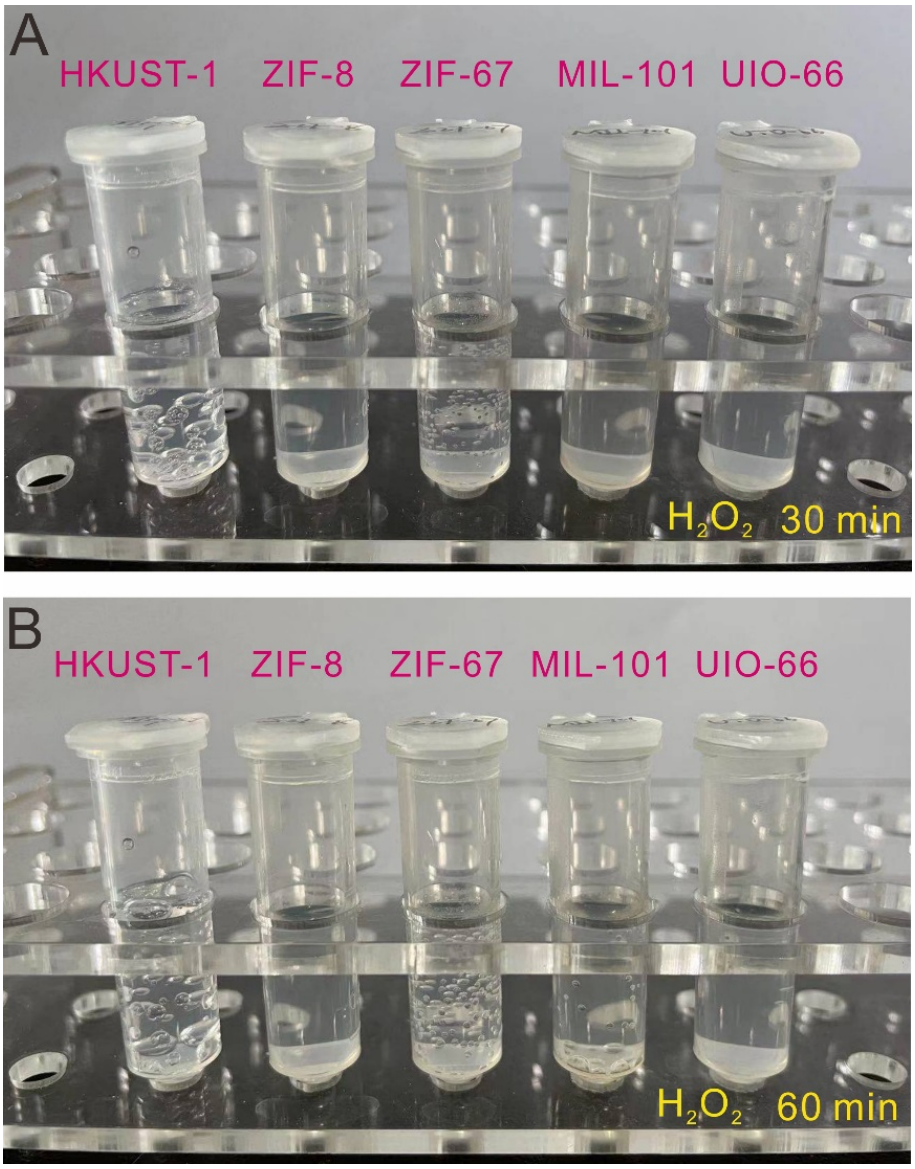

Figure S4. Photographs of tubes containing five types of MOFs in 10 M H_2O_2 solution at 37 ºC for (A) 30 min and (B) 60 min.

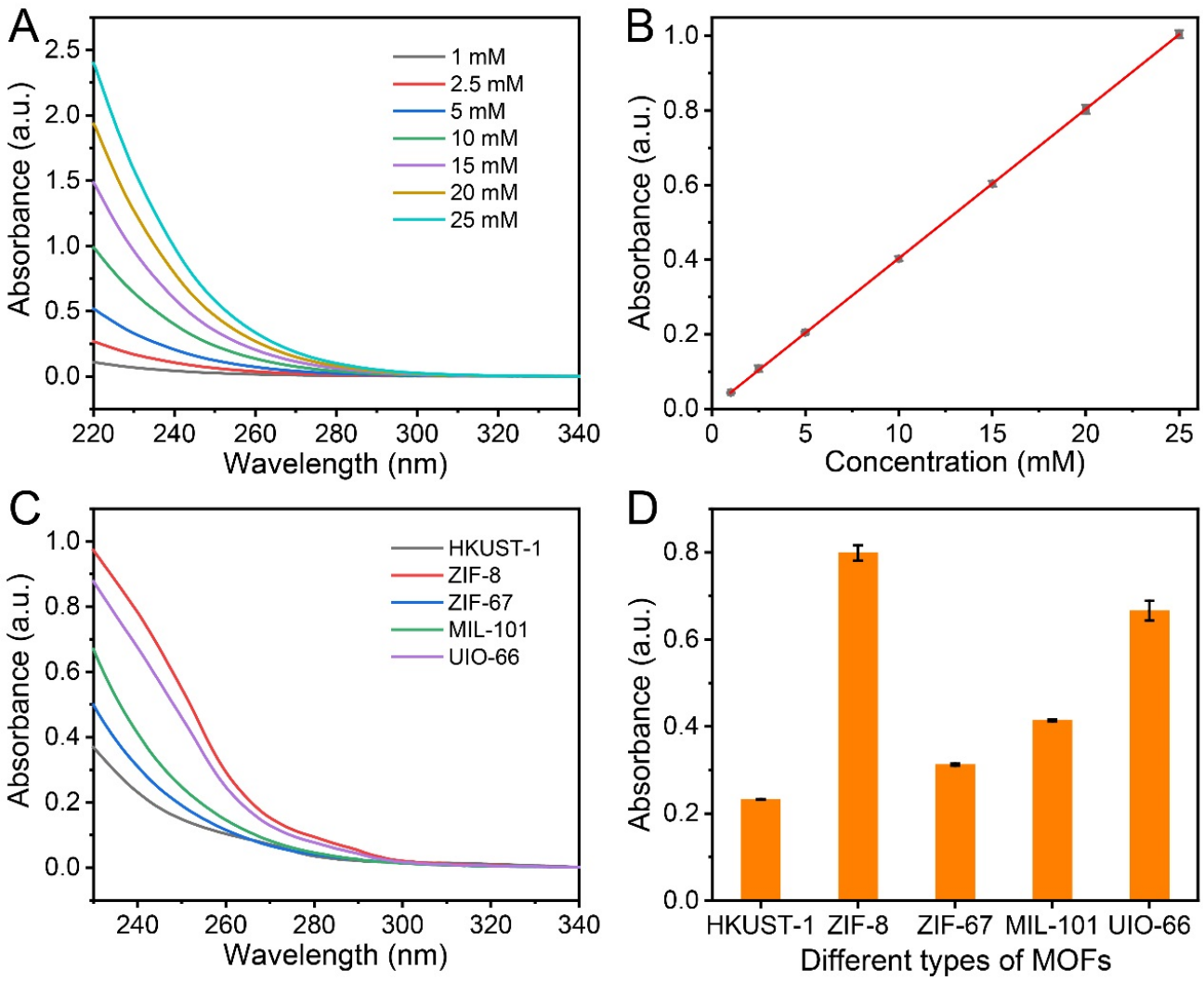

Figure S5. (A) UV-Vis spectra of different concentrations of H_2O_2 (1, 2.5, 5, 10, 15, 20, and 25 mM). (B) The calibration curve of absorbance at 240 nm and the concentration of H_2O_2. (C) UV−Vis spectra and (D) absorbance of remainder H_2O_2 were recorded after reaction with five types of MOFs for 60 min.

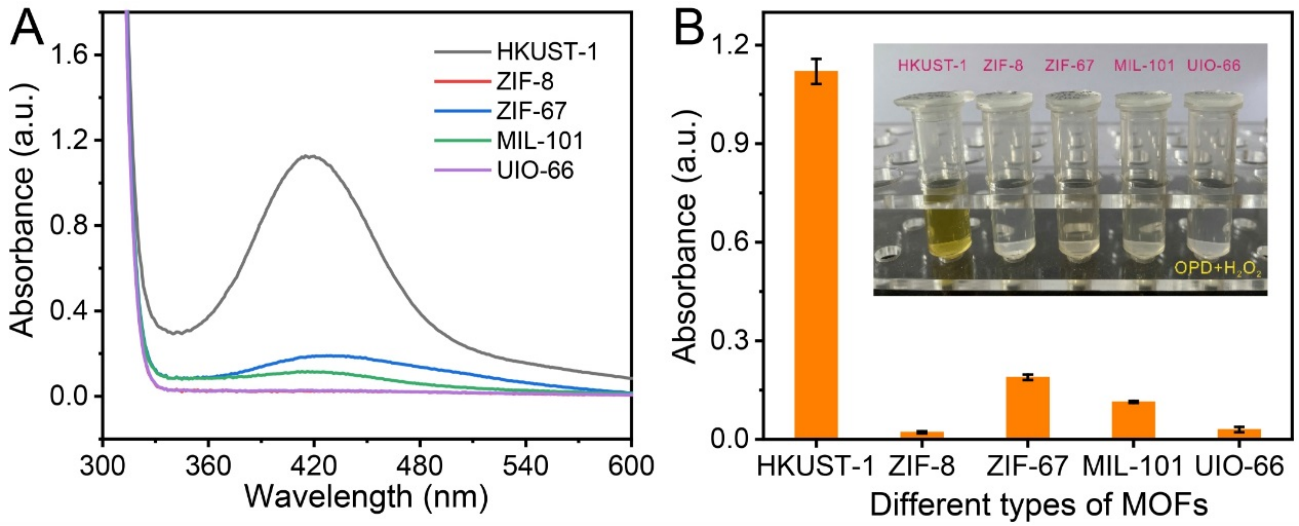

Figure S6. (A) UV-Vis spectra and (B) absorbance of five different types of MOFs after reaction with 10 mM OPD and 8 mM H_2O_2 for 10 min. The inset exhibits the photographs of five different types of MOFs added to a mixture of OPD and H_2O_2.

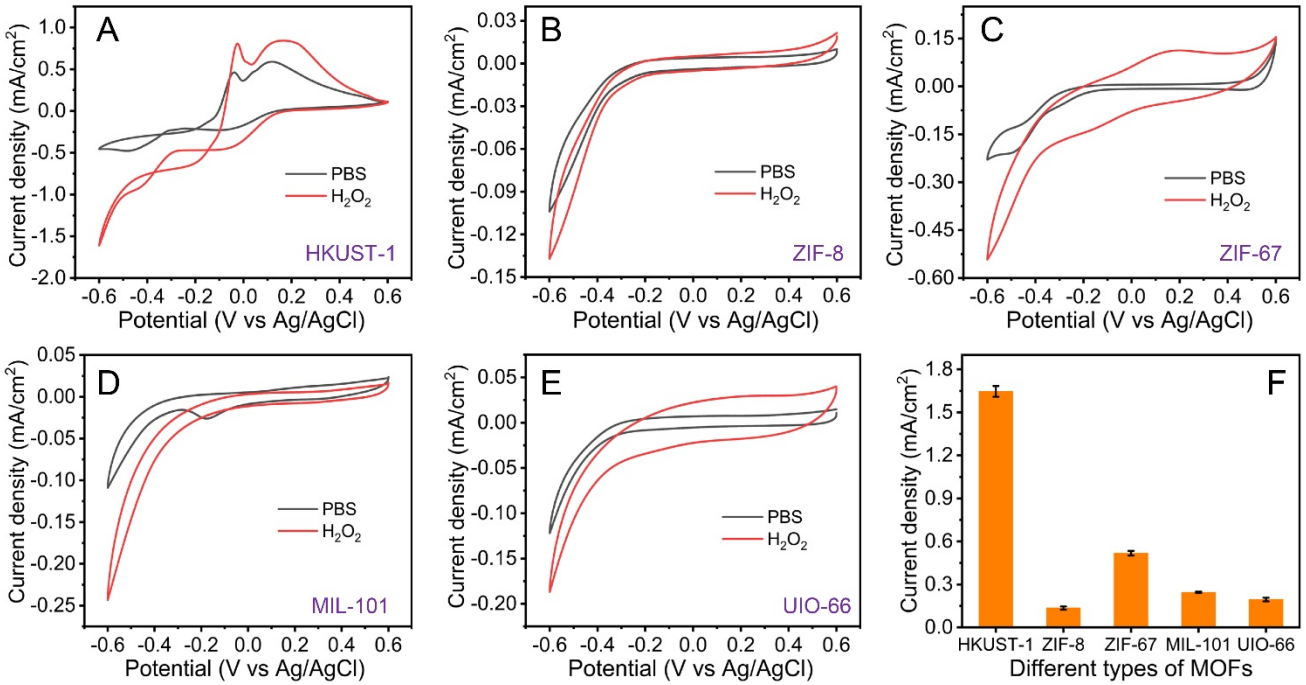

Figure S7. (A-E) CVs and (F) current density of (A) HKUST-1/GCE, (B) ZIF-8/GCE, (C) ZIF-67/GCE, (D) MIL-101/GCE, and (E) UIO-66/GCE in 10 mM PBS with 3 mM H_2O_2.

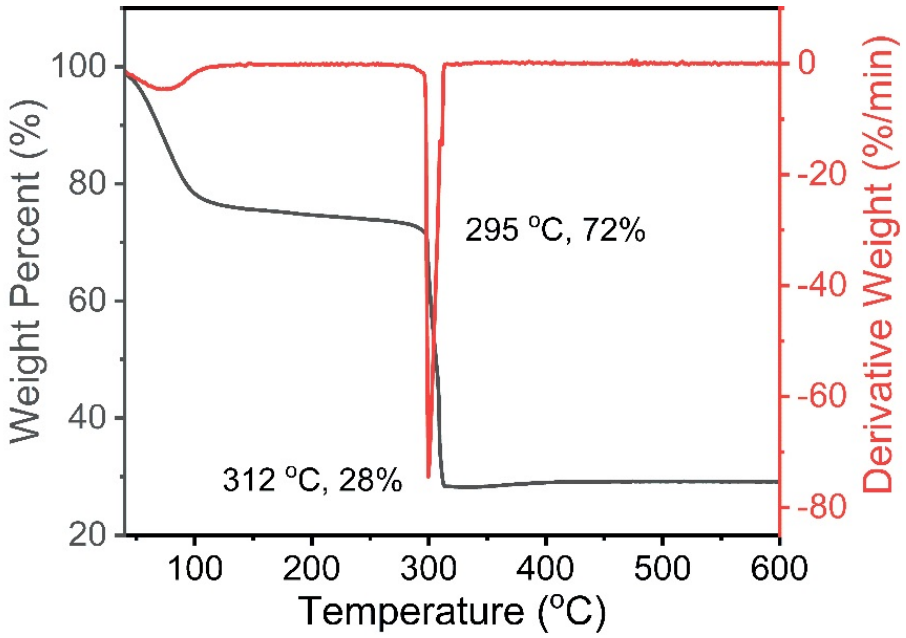

Figure S8. TGA analysis curve of HKUST-1 under air atmosphere, revealing optimal calcination temperature region where Cu dimer distortion is possible while maintaining the MOF structure.

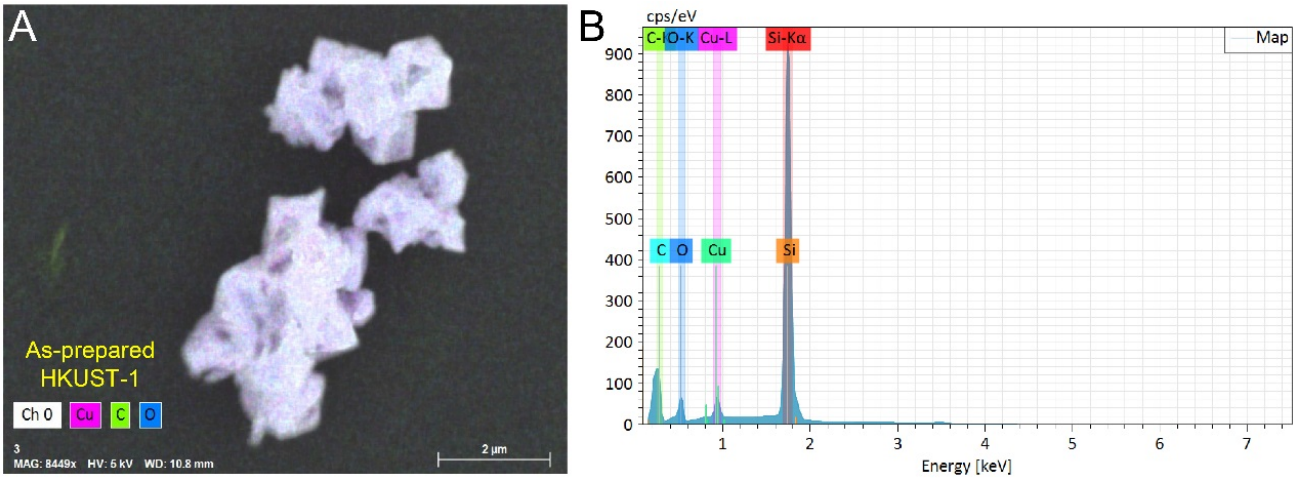

Figure S9. EDS mapping analysis of as-prepared HKUST-1.

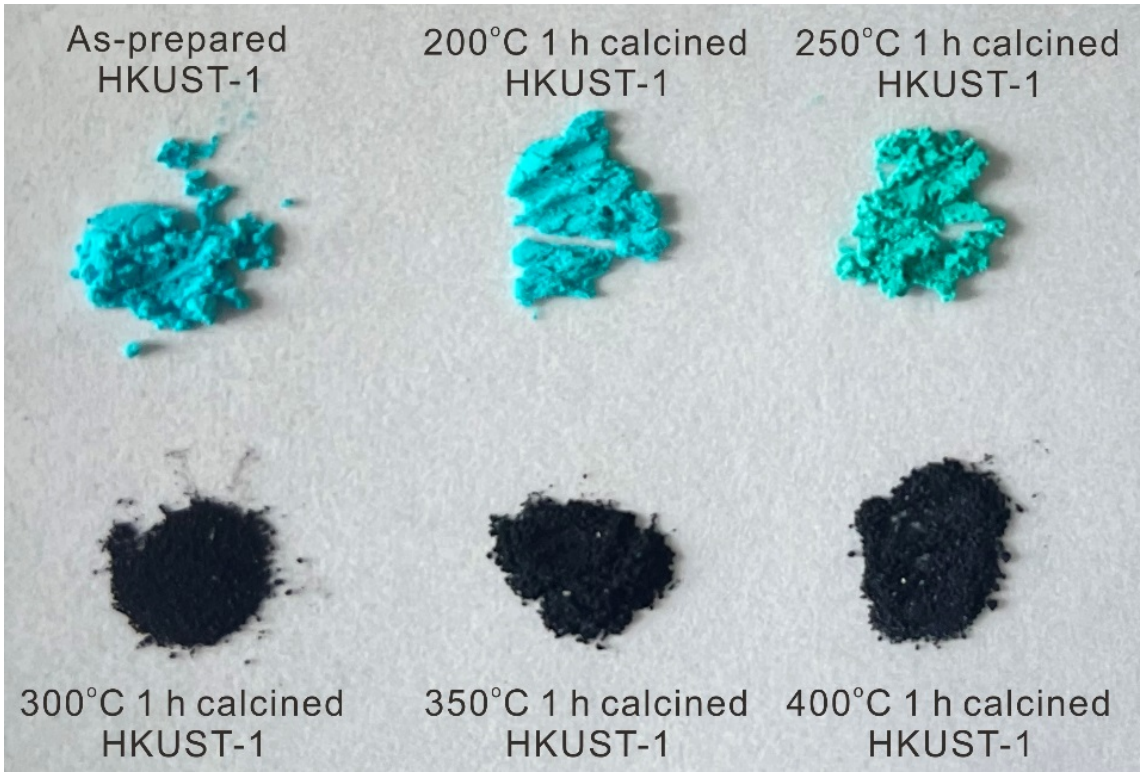

Figure S10. HKUST-1 powders (as-prepared, 200ºC, 250ºC, 300ºC, 350ºC, and 400ºC calcination) fabricated in this work.

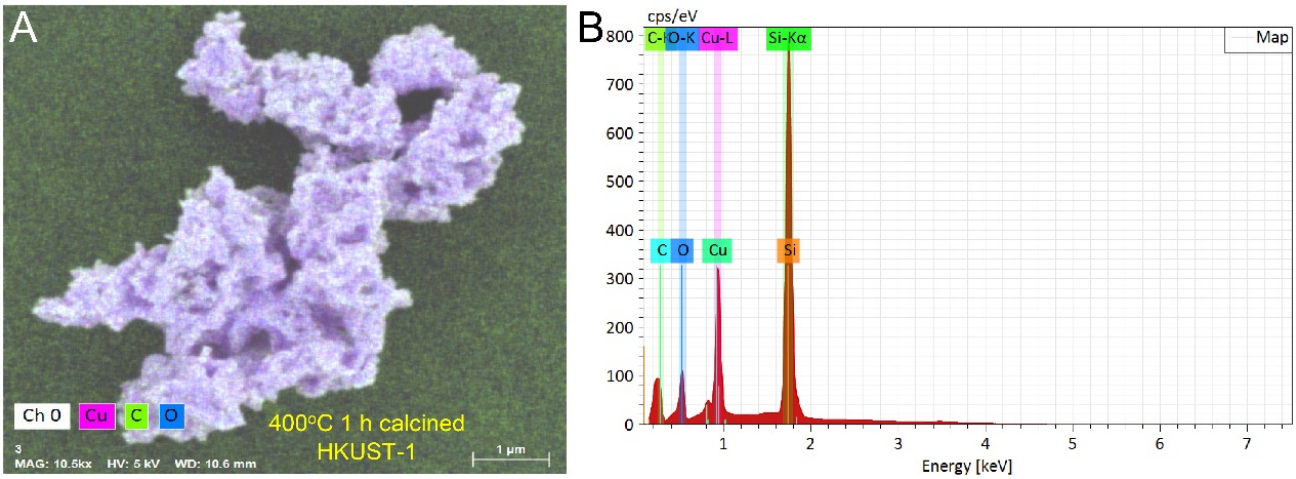

Figure S11. EDS mapping analysis of the calcined HKUST-1 at 400ºC for 1 h.

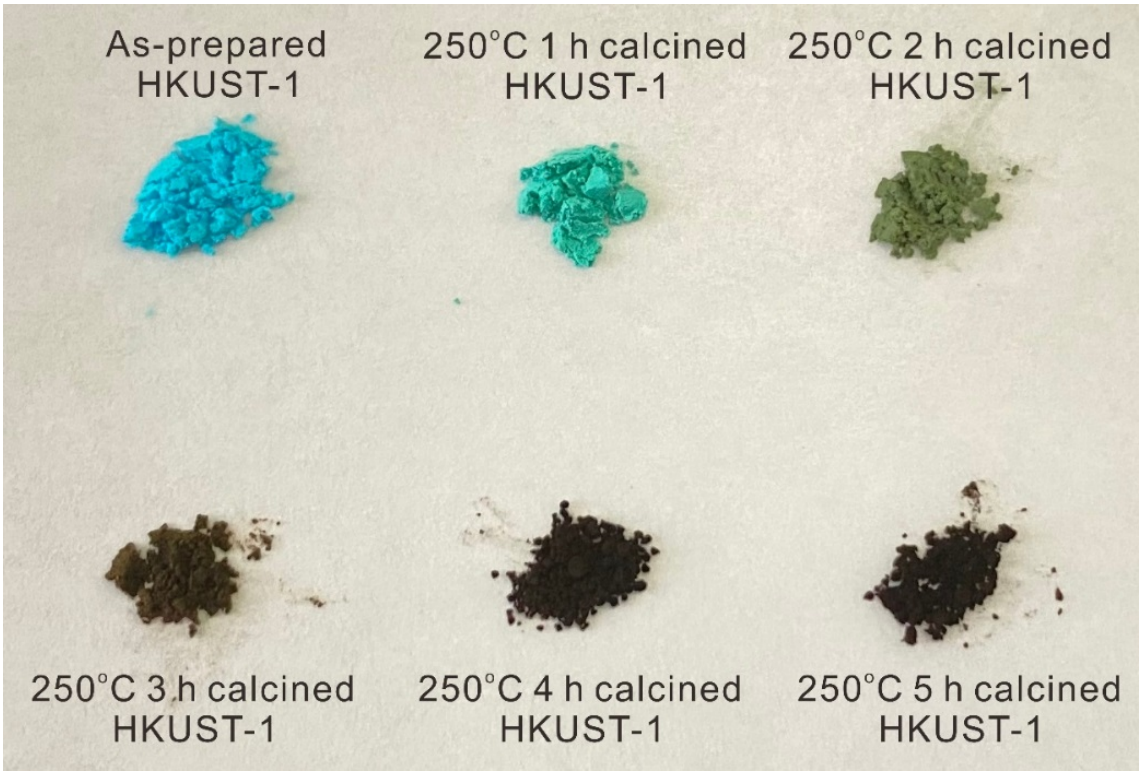

Figure S12. HKUST-1 powders (as-prepared, 1, 2, 3, 4, and 5 h calcination at 250°C) fabricated in this work.

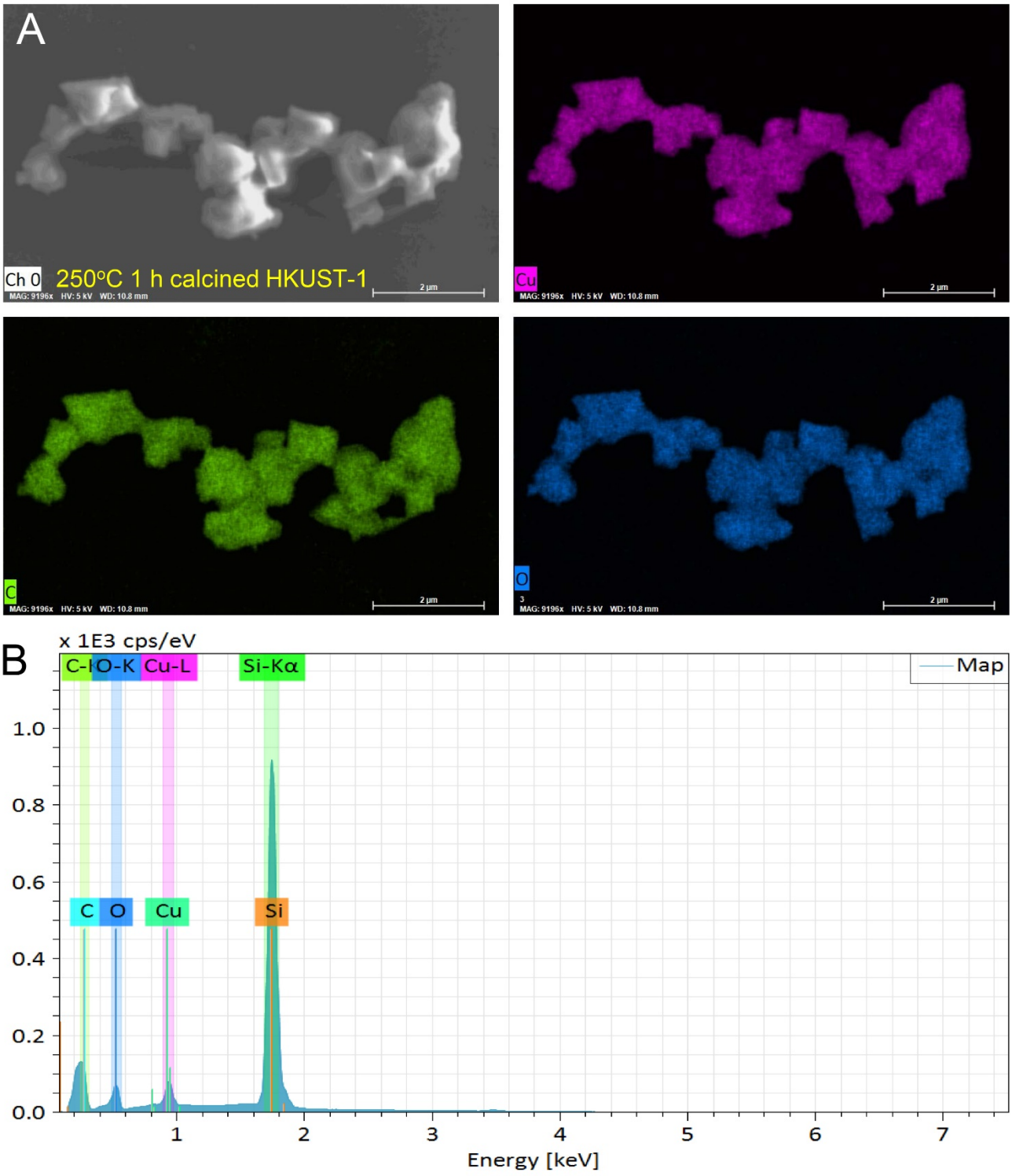

Figure S13. EDS mapping analysis of the calcined HKUST-1 at 250ºC for 1 h.

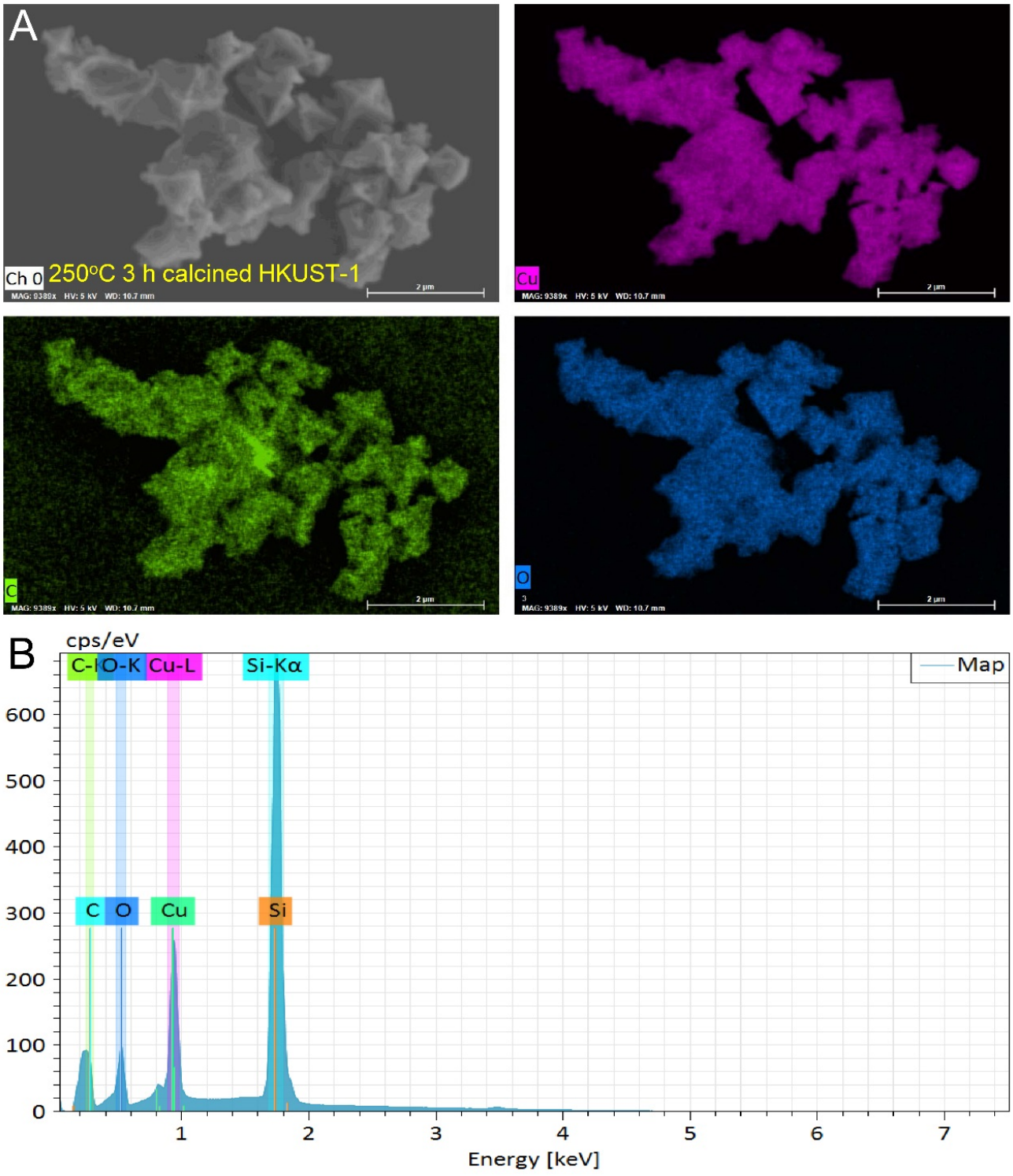

Figure S14. EDS mapping analysis of the calcined HKUST-1 at 250ºC for 3 h.

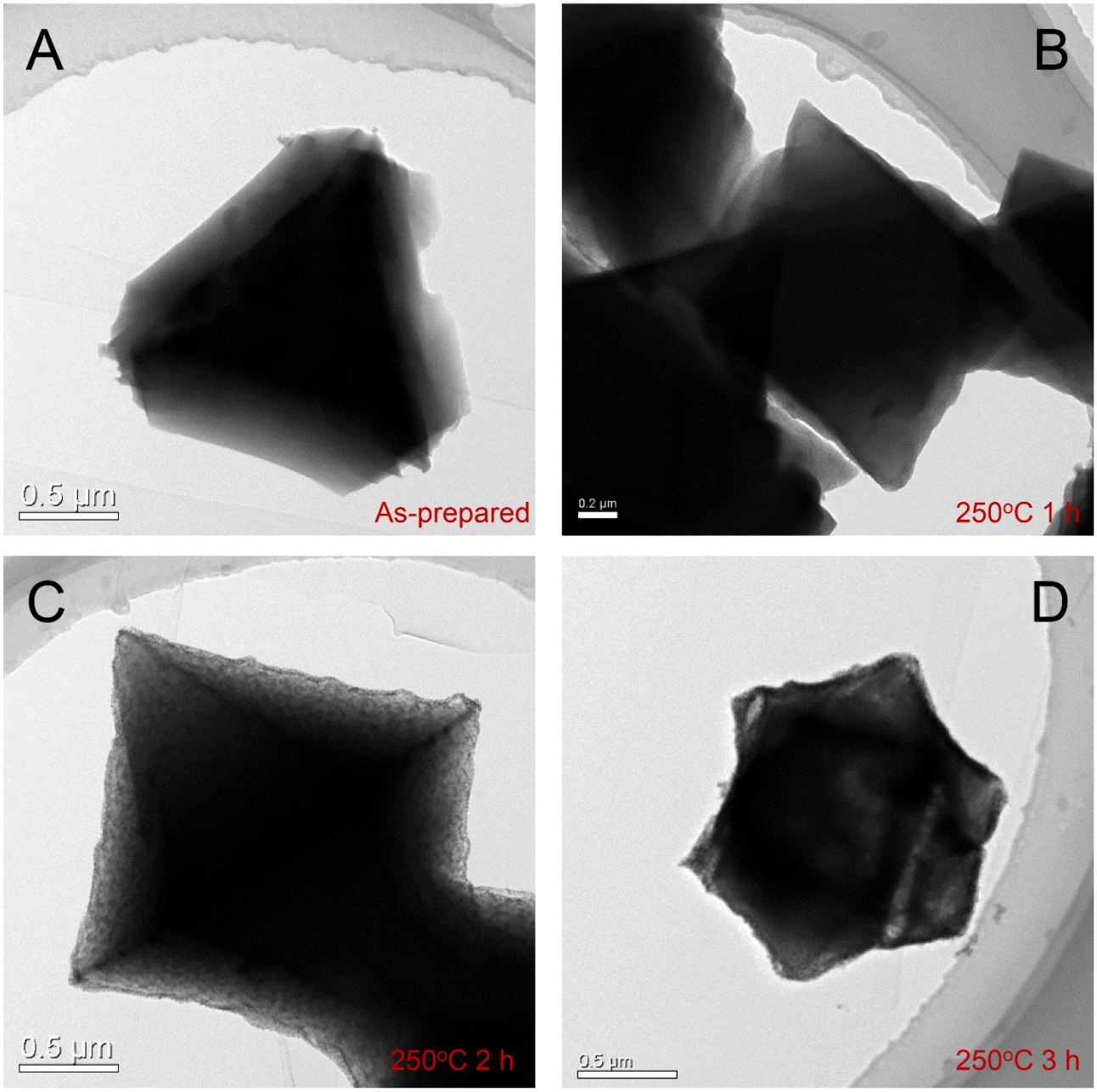

Figure S15. TEM images of the (A) as-prepared HKUST-1 and calcined HKUST-1 at 250°C for (B) 1, (C) 2, and (D) 3 h.

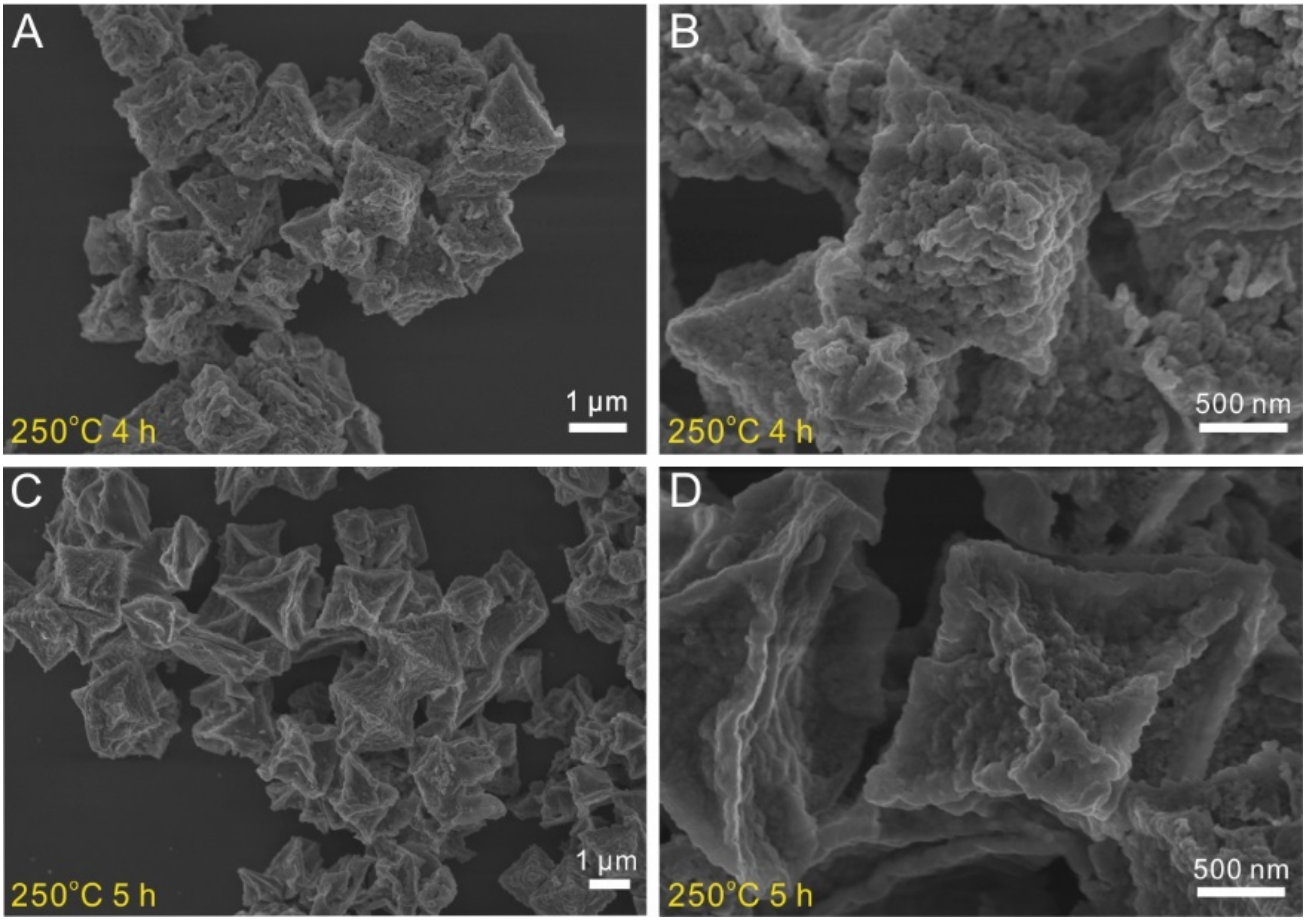

Figure S16. SEM images of the calcined HKUST-1 at 250ºC for (A and B) 4 h and (C and D) 5 h.

Table S2 Elemental quantification of as-prepared HKUST-1, HKUST-1 (250 ºC, 1 h), HKUST-1 (250 ºC, 2 h), HKUST-1 (250 ºC, 3 h), HKUST-1 (250 ºC, 4 h), and HKUST-1 (250 ºC, 5 h) determined by XPS spectra.

Samples	C/at%	O/at%	N/at%	Cu/at%
HKUST-1	75.84	20.08	1.64	2.45
HKUST-1 (250 ºC, 1 h)	58.75	31.28	0.98	9
HKUST-1 (250 ºC, 2 h)	57.73	32.03	0.63	9.61
HKUST-1 (250 ºC, 3 h)	58.71	27.67	1.02	12.6
HKUST-1 (250 ºC, 4 h)	43.38	33.81	0.83	21.99
HKUST-1 (250 ºC, 5 h)	34.3	38.38	0.84	26.48

Table S3 The atomic ratio of C:Cu, O:Cu, and Cu:N for as-prepared HKUST-1, HKUST-1 (250 ºC, 1 h), HKUST-1 (250 ºC, 2 h), HKUST-1 (250 ºC, 3 h), HKUST-1 (250 ºC, 4 h), and HKUST-1 (250 ºC, 5 h) determined by XPS spectra.

Samples	C:Cu	O:Cu	Cu:N
HKUST-1	30.9	8.20	1.49
HKUST-1 (250 ºC, 1 h)	6.53	3.47	9.18
HKUST-1 (250 ºC, 2 h)	6.00	3.33	15.2
HKUST-1 (250 ºC, 3 h)	4.66	2.20	12.3
HKUST-1 (250 ºC, 4 h)	1.97	1.54	26.5
HKUST-1 (250 ºC, 5 h)	1.29	1.45	31.5

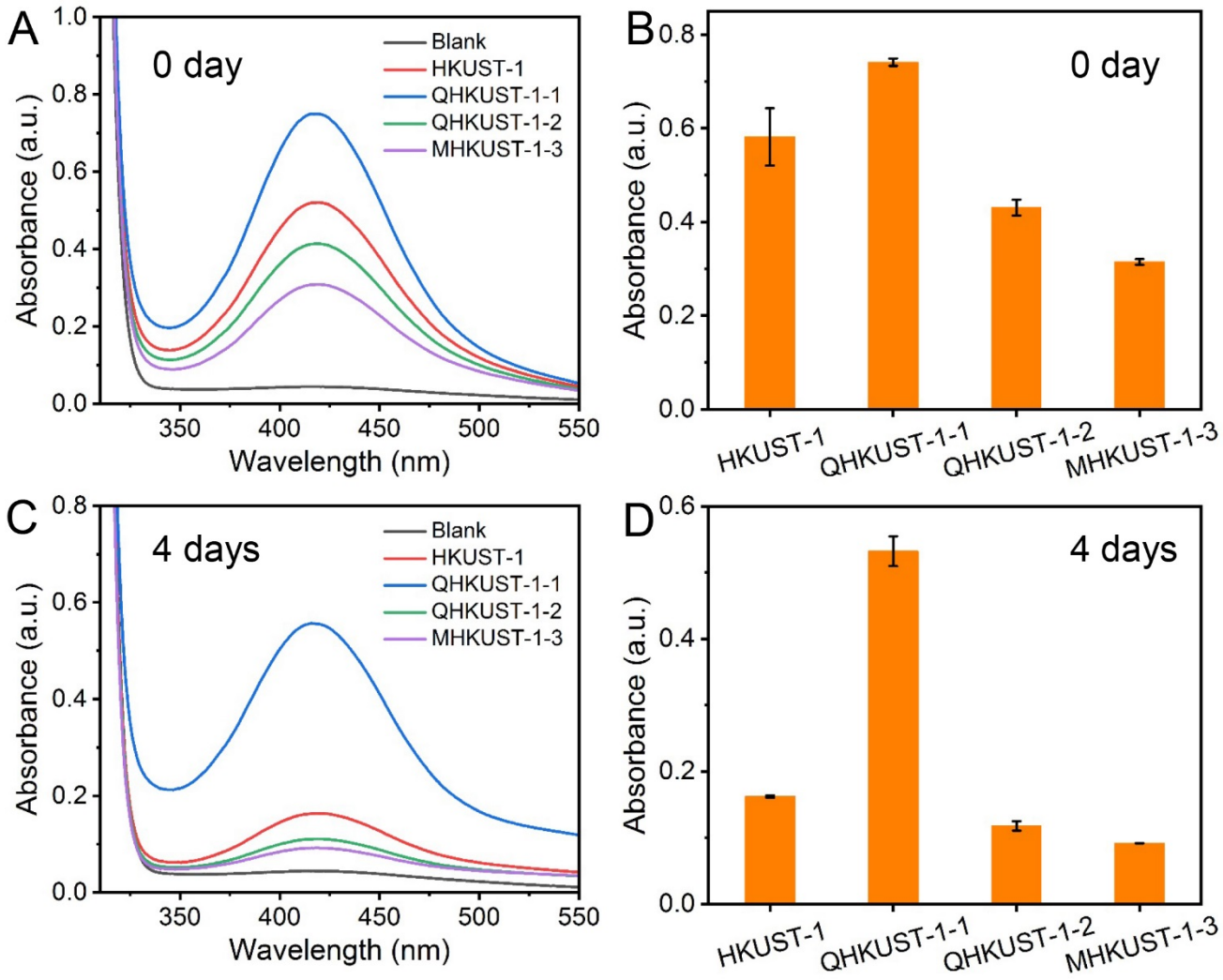

Figure S17. UV-Vis absorbance of HKUST-1 and QHKUST-1 after reaction with H_2O_2 and OPD solution (A and B) before and (C and D) after 4 days of the hydrostability test.

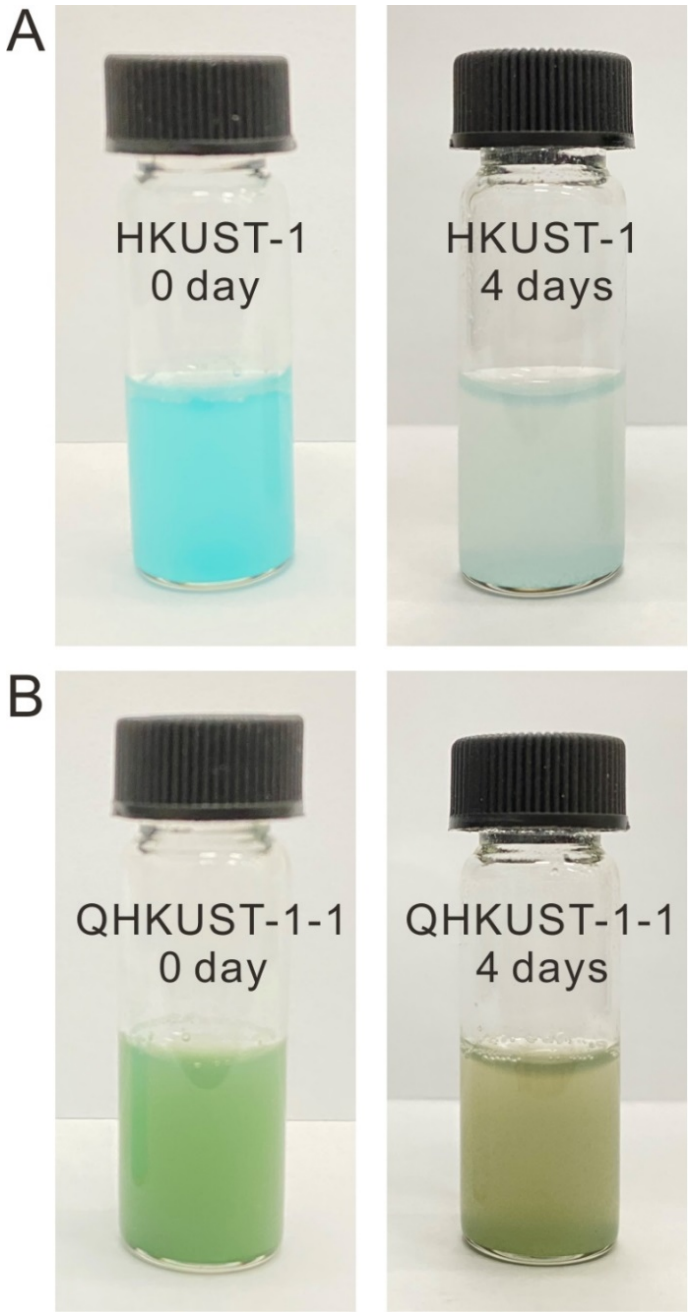

Figure S18. Digital photographs of (A) HKUST-1 and (B) QHKUST-1-1 water solution before and after 4 days of hydrostability test.

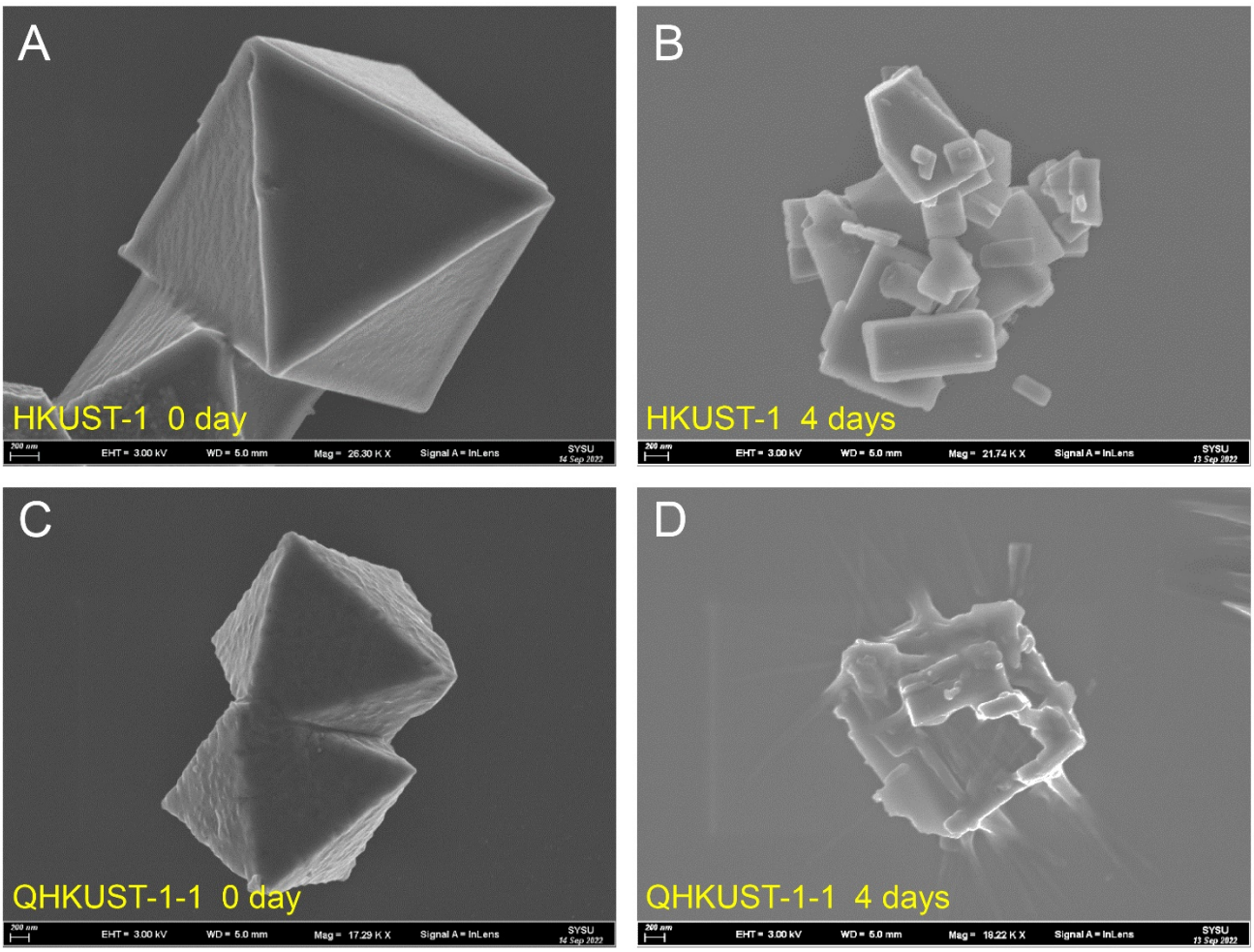

Figure S19. SEM images of (A and B) HKUST-1 and (C and D) QHKUST-1-1 before and after 4 days of hydrostability test.

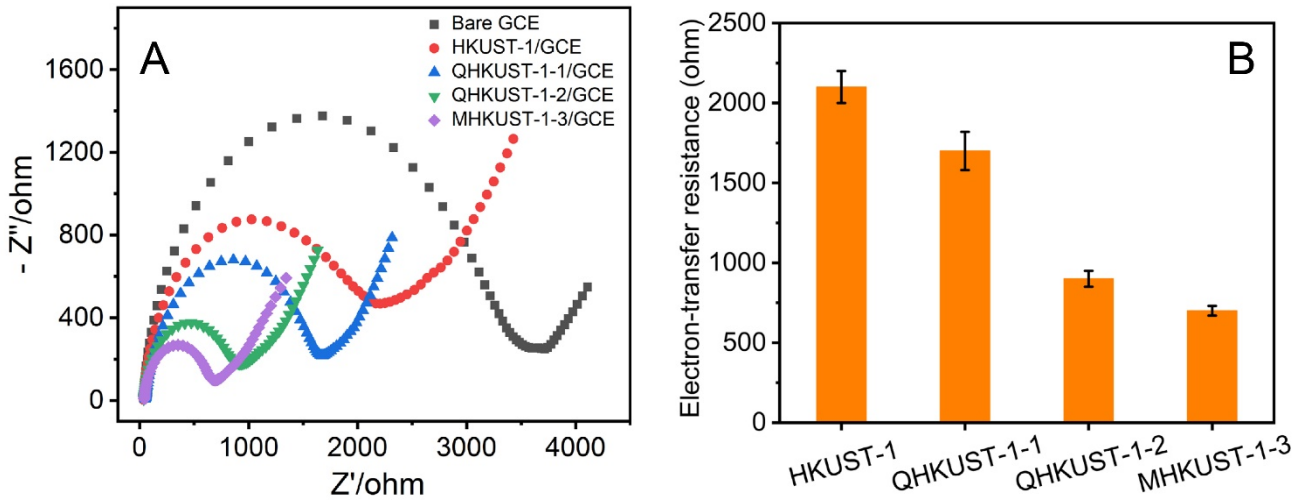

Figure S20. (A) EIS and (B) electro-transfer resistance of as-prepared HKUST-1 and calcined HKUST-1 at 250ºC for 1, 2, and 3 h in 0.5 M KCl solution containing 5 mM $[Fe(CN)_6]^{4-/3-}$ (impedance spectral frequency 0.1–10^5 Hz, amplitude 10mV).

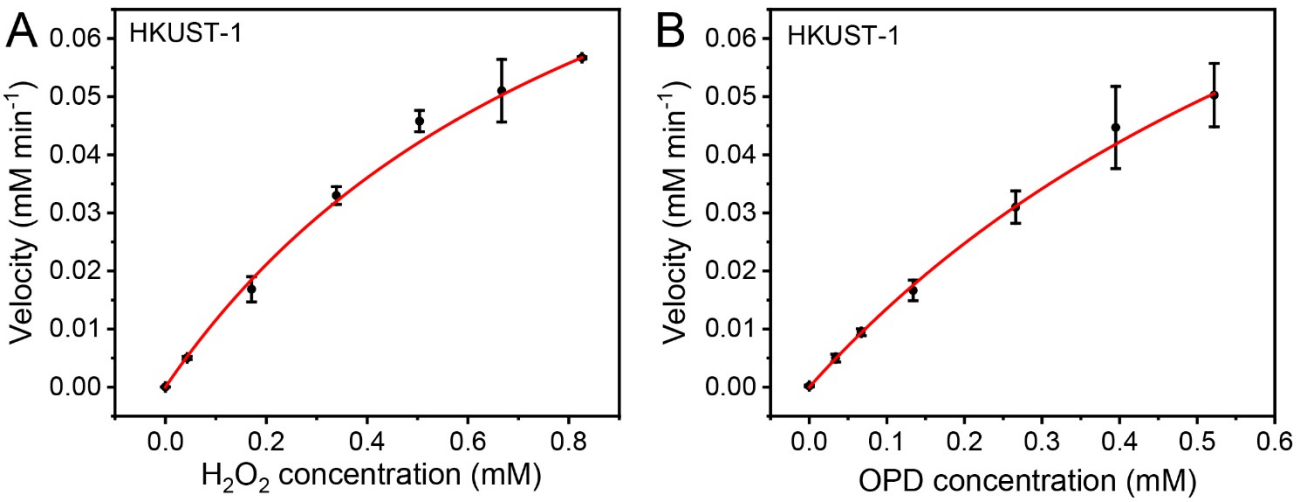

Figure S21. Results of Michaelis−Menten curves for (A) H_2O_2 and (B) OPD by HKUST-1.

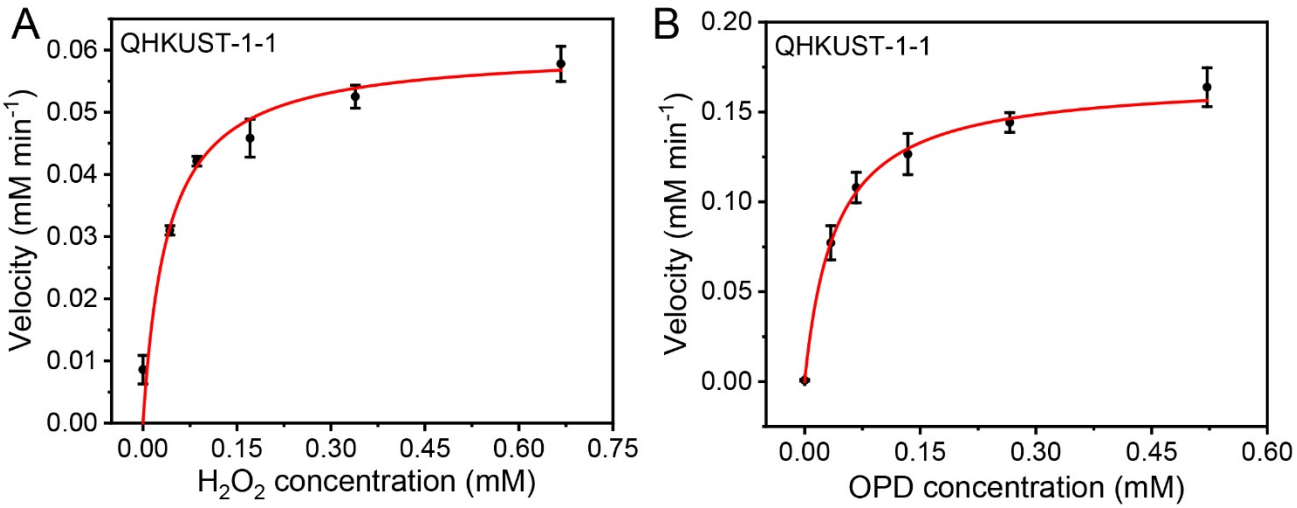

Figure S22. Results of Michaelis−Menten curves for (A) H_2O_2 and (B) OPD by QHKUST-1.

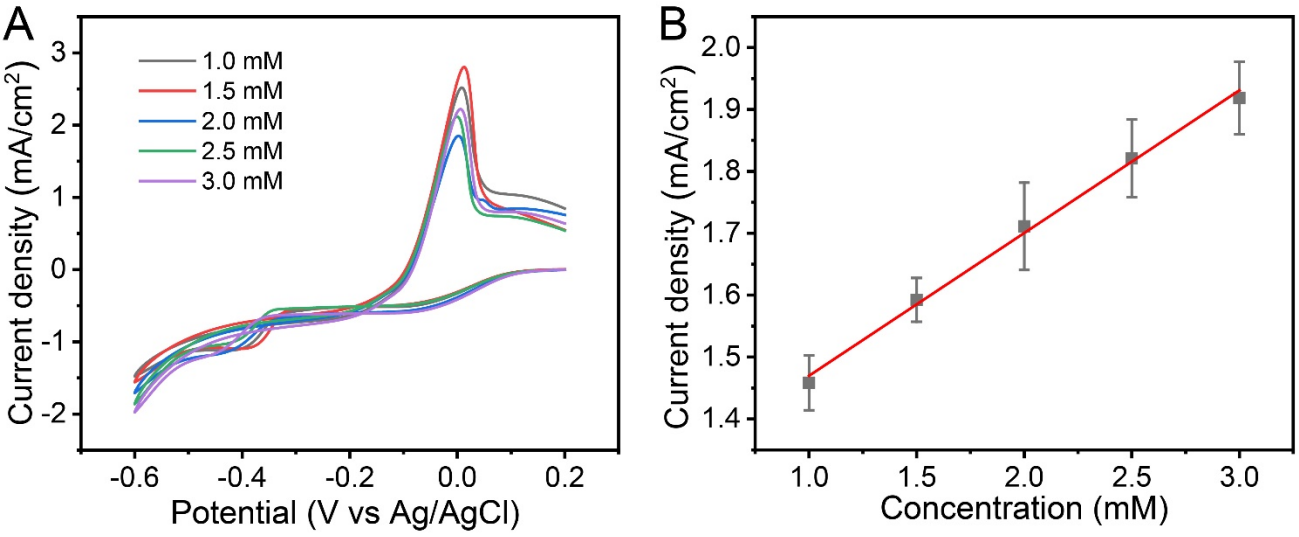

Figure S23. (A) CVs of QHKUST-1/GCE in 10 mM PBS with different H_2O_2 concentrations (1, 1.5, 2, 2.5, and 3 mM). (B) Calibration curve of the current density to the concentration of H_2O_2 from 1 mM to 3 mM.

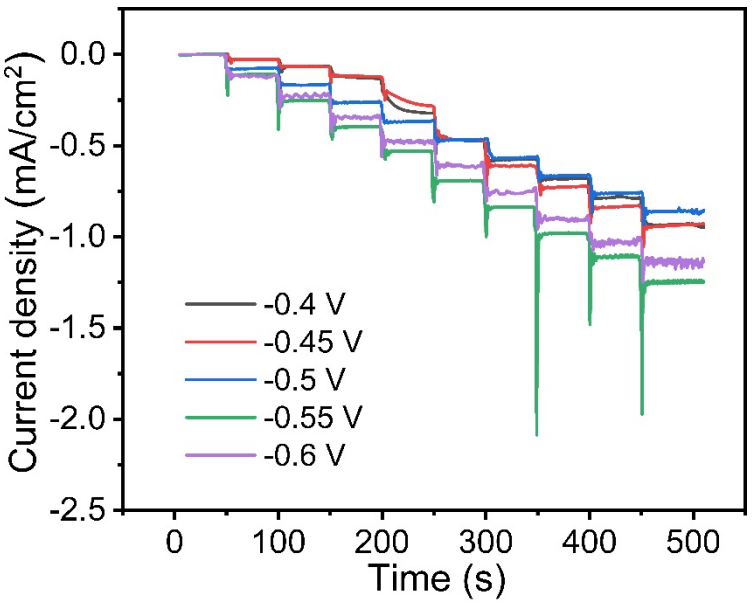

Figure S24. Electrochemical responses of QHKUST-1 modified GCE at various potentials (vs Ag/AgCl) with the successive addition of 0.2 mM H_2O_2.

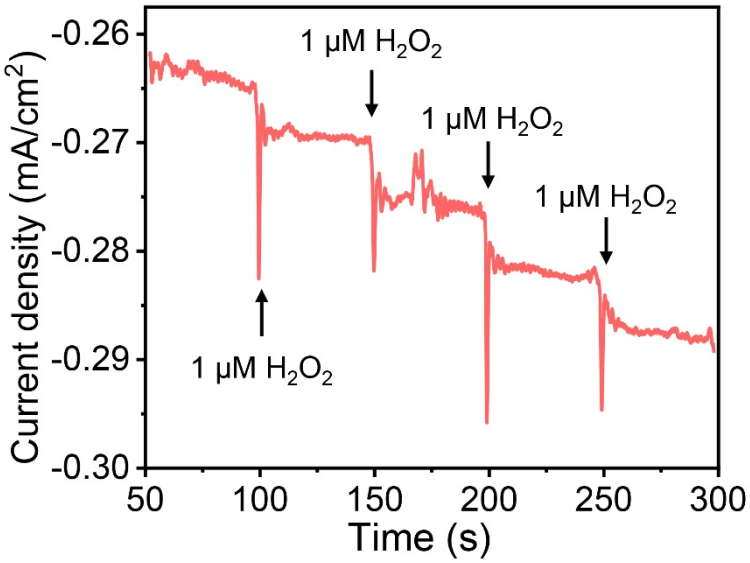

Figure S25. Electrochemical responses of QHKUST-1 modified GCE with the successive addition of 1 μM H_2O_2.

Table S4. Comparison of the detection performance of different H_2O_2 sensors.

Materials	Linear range (μM)	Detection Limit (μM)	Reference
HKUST-1/GCE	2-25,000	0.68	1
Hemin/Cu-MOF/GCE	10-5,000	4.14	2
Ag/H-ZIF-67/GCE	5−67,000	1.1	3
AuNPs-NH_2/Cu-MOF/GCE	5–850	1.2	4
AuNP/Hb-HKUST-1/GCE	0.15-2.4	0.731	5
CS-SGO@HKUST-1/GCE	1−5,600	0.49	6
QHKUST-1/GCE	1-11,000	0.3	This work

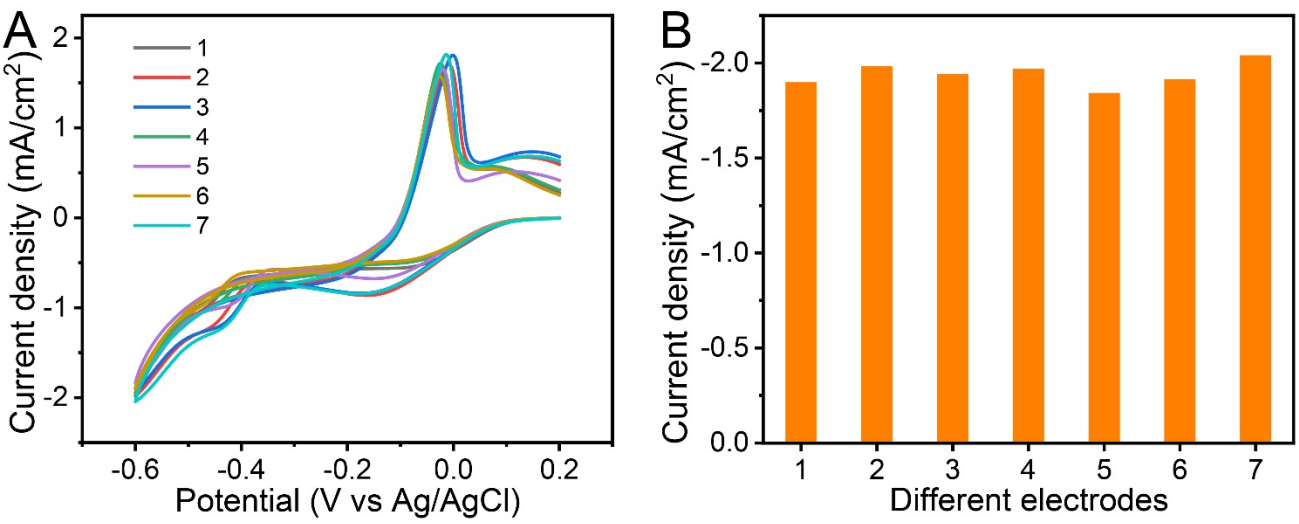

Figure S26. Current density of different QHKUST-1/GCEs prepared under the same conditions in PBS solution containing 3 mM H_2O_2.

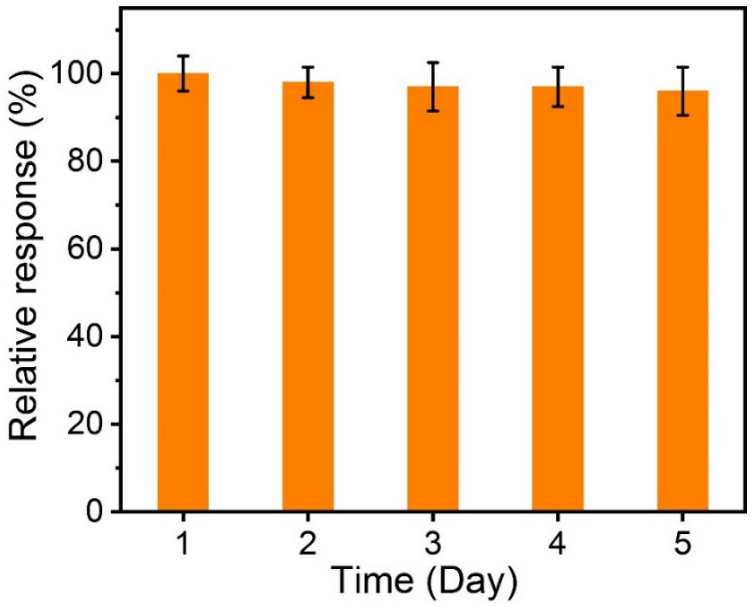

Figure S27. Stability test of the QHKUST-1/GCE over five days.

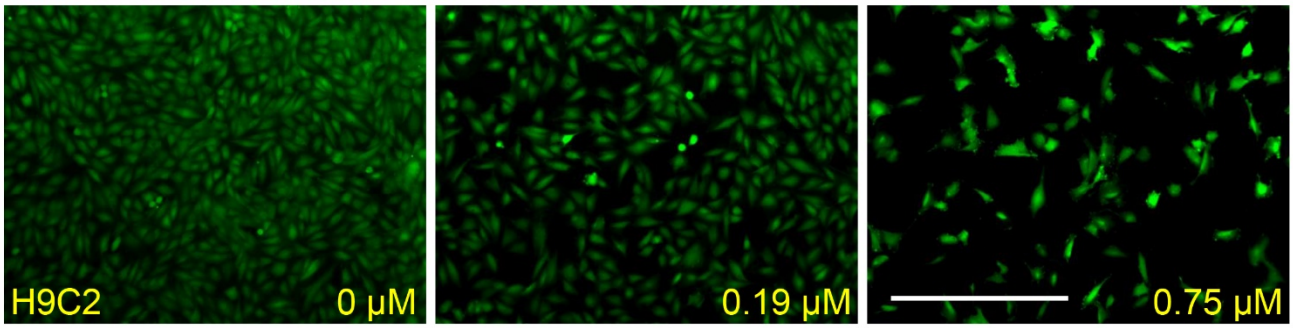

Figure S28. Fluorescence images of H9C2 cells stained by calcein-AM with different concentrations of DOX. (Scale bar: 200 μm)

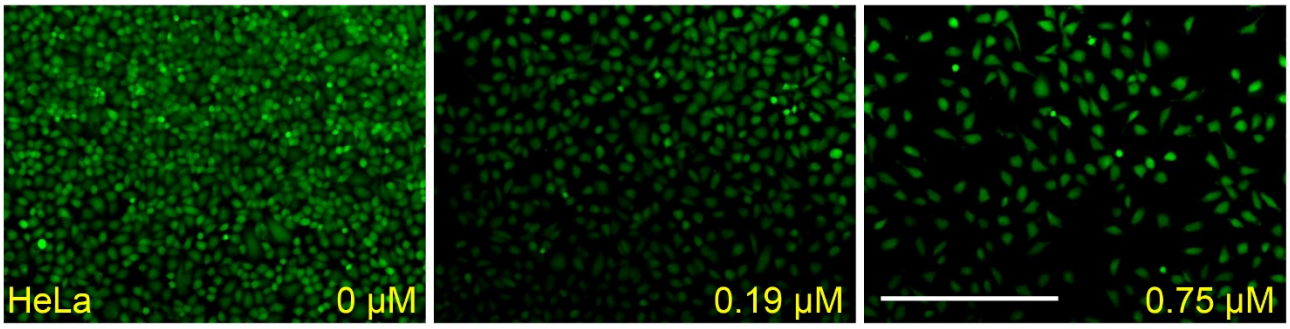

Figure S29. Fluorescence images of HeLa cells stained by calcein-AM with different concentrations of DOX. (Scale bar: 200 μm)

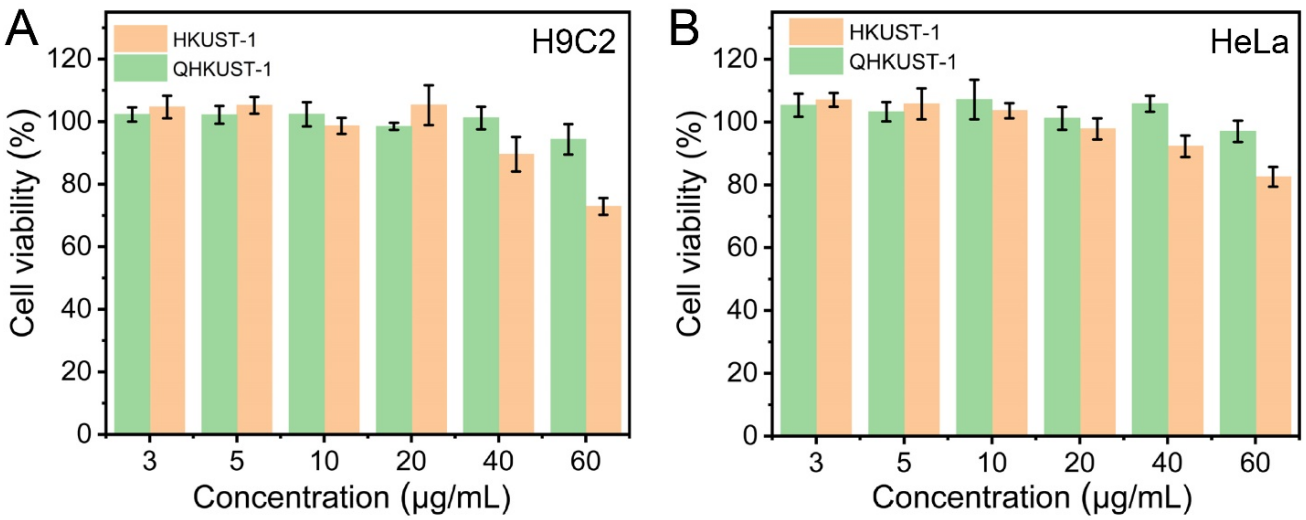

Figure S30. Cell viability of (A) H9C2 cells and (B) HeLa cells using a CCK-8 assay incubated with different concentrations of HKUST-1 and QHKUST-1.

3. Supplementary References

1. X. J. Guo, C. Y. Lin, M. J. Zhang, X. W. Duan, X. R. Dong, D. P. Sun, J. B. Pan and T. H. You, *Frontiers in Chemistry*, 2021, **9**, 743637.
2. H. Cui, S. S. Cui, S. Y. Zhang, Q. J. Tian, Y. F. Liu, P. Zhang, M. X. Wang, J. L. Zhang and X. J. Li, *Analyst*, 2021, **146**, 5951-5961.
3. D. P. Sun, D. C. Yang, P. Wei, B. Liu, Z. G. Chen, L. Y. Zhang and J. Lu, *ACS Applied Materials & Interfaces*, 2020, **12**, 41960-41968.
4. W. J. Dang, Y. M. Sun, H. Jiao, L. Xu and M. Lin, *Journal of Electroanalytical Chemistry*, 2020, **856**, 113592.
5. Q. Wang, J. Gong, Q. Q. Bai, Y. L. Qin, X. B. Zhou, M. M. Wu, H. W. Ji and L. Wu, *Journal of Materials Chemistry B*, 2021, **9**, 4002-4005.
6. Q. X. Wang, Y. Z. Yang, F. Gao, J. C. Ni, Y. H. Zhang and Z. Y. Lin, *Acs Applied Materials & Interfaces*, 2016, **8**, 32477-32487.